ELECTRONIC SUPPLEMENTAL INFORMATION

Vibrational Spectroscopy Investigation of Defects in Zr- and Hf-UiO-66

Brandon T. Yost*, Bradley Gibbons†, Addison Wilson*, Amanda J. Morris†, L.E. McNeil*

* Department of Physics and Astronomy, University of North Carolina, Chapel Hill North Carolina.

† Department of Chemistry, Virginia Polytechnic Institute and State University, Blacksburg, Virginia.
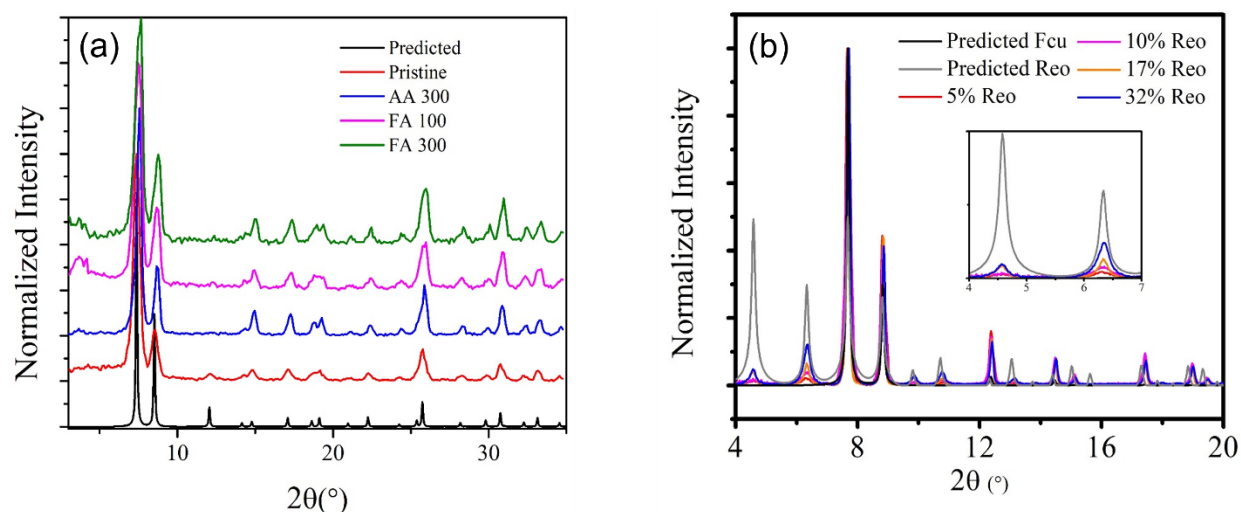
Powder X-ray Diffraction

Figure S1: **(a)** X-ray diffraction pattern for Zr-UiO-66 sample series. **(b)** X-ray diffraction pattern for all Hf-UiO-66 samples. The inset image shows the two low-angle peaks which correspond to the emergence of the **reo** topology.

PXRD was obtained on a Rigaku MiniFlex diffractometer with Cu Kα radiation (λ = 1.5418 Å). The samples were analyzed using a 15 °/minute continuous scanning mode with 0.1 ° resolution from 3 to 50° 2θ. For Hf-UiO-66 samples, the percent **reo** fitting was obtained by fitting the predicted patterns for fcu and reo UiO-66 from 4-9 ° 2θ to get the best fit of the four primary peaks[18].

PXRD patterns for the Hf-UiO-66 samples were fit by a linear combination of the predicted patterns of **reo** and **fcu** UiO-66. The experimental patterns were normalized, and the fitting was performed on the first four peaks to give a percentage of **reo** in the sample. While PXRD has been previously used in the literature to measure missing cluster defects present in the **reo** phase there are some significant limitations to this approach. To start, peaks at low angles are difficult to resolve on most benchtop diffractometers, often appearing as a single broad peak which is not easy to fit with predicted patterns. Furthermore, the intensity of these peaks is related to both the number of missing

clusters, and the correlation of these defects to form nanoregions of a new crystal phase. The relative size of these nanoregions impact the intensity of **reo** peaks, meaning two samples with the same number of missing cluster defects may have different PXRD intensities depending on the location of these defects within the MOF particle. Recognizing these limitations, PXRD is still the primary method of detecting missing cluster defects and **reo** phase UiO-66 and these fittings provide a rough estimation of the number of missing clusters in the sample.
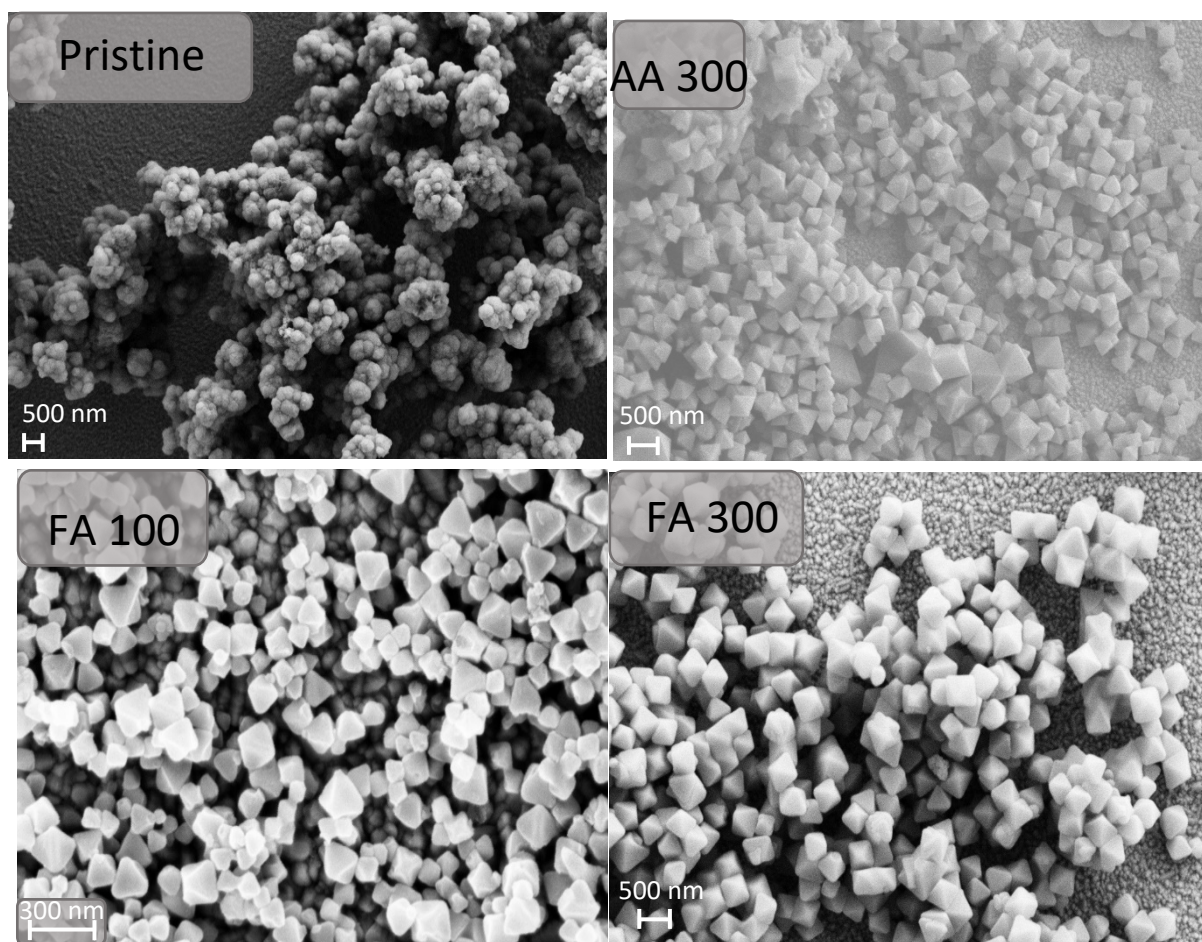
Scanning electron microscopy
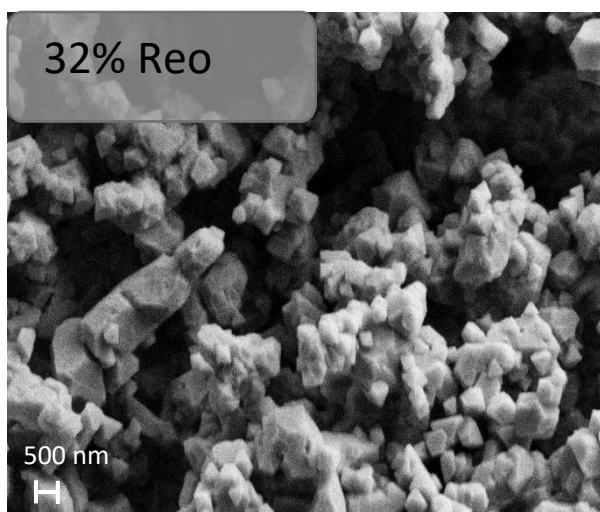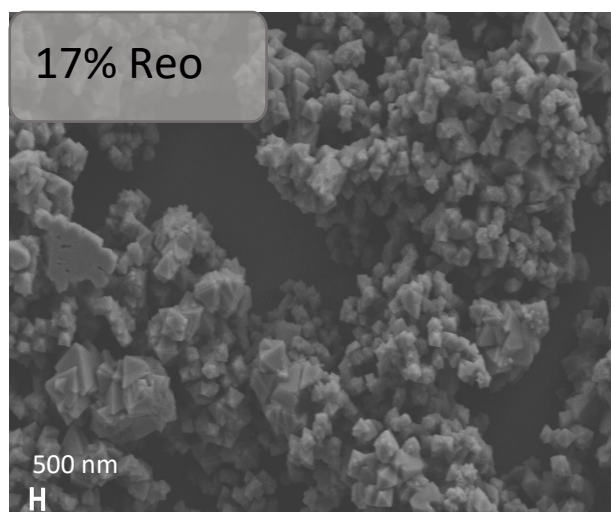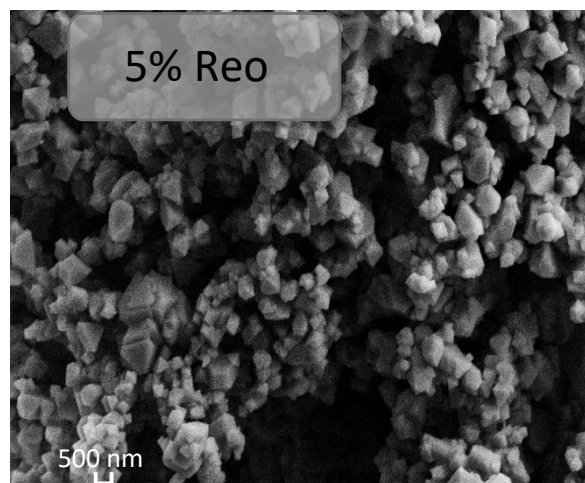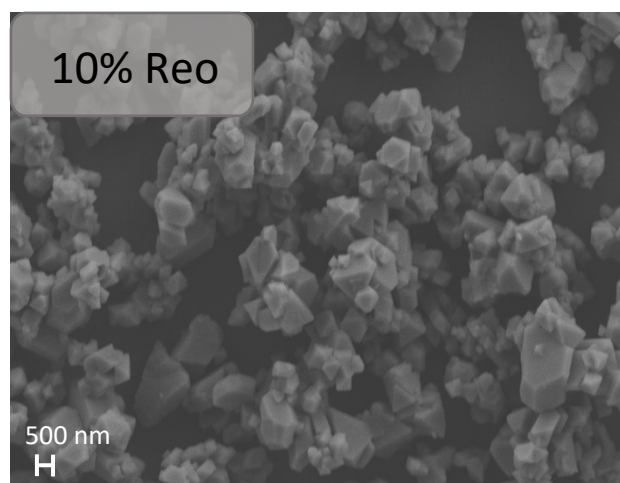

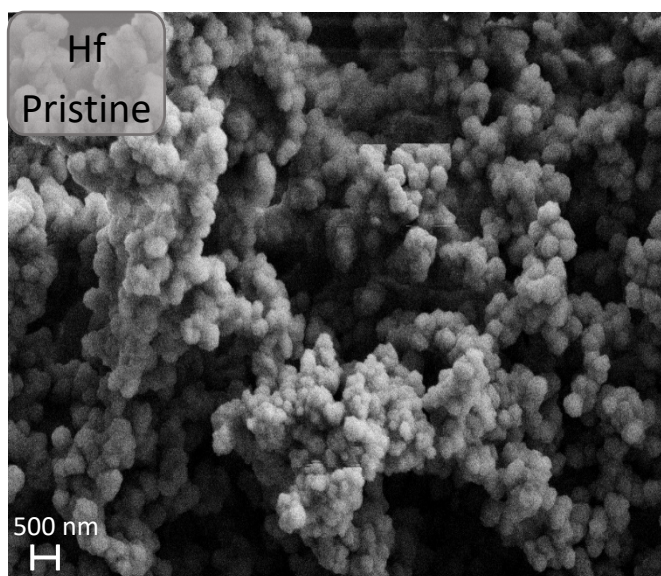**Figure S2**: SEM images for Zr-UiO-66.

Figure S3: SEM images forHf-UiO-66.

SEM was collected using a LEO/Zeiss 1550 field emission scanning electron microscope. Samples were prepared by drop casing from a methanol suspension onto a fluorine doped tin oxide (FTO) slide. These images were used to calculate the particle size of each sample.

Samples	Defect Level (%)	Particle Size (nm)
Zr Pristine	0.9 ± 2	440 ± 70
AA 300	14 ± 2	595 ± 120
FA 100	22 ± 2	137 ± 40
FA 300	24 ± 2	635 ± 110
Hf Pristine	0.9	400 ± 70
5% Reo	N/A	1200 ± 450
10% Reo	N/A	1580 ± 570
17% Reo	N/A	2270 ± 550
32% Reo	N/A	590 ± 130

Table S1: Defect level and Particle size data for all relevant samples. For all Zr–UiO-66 samples, defect density was calculated via TGA whereas the defect density of Hf-UiO-66 (% reo) was extracted from fits of the two low angle peaks in the PXRD data. Particle size is calculated from SEM.

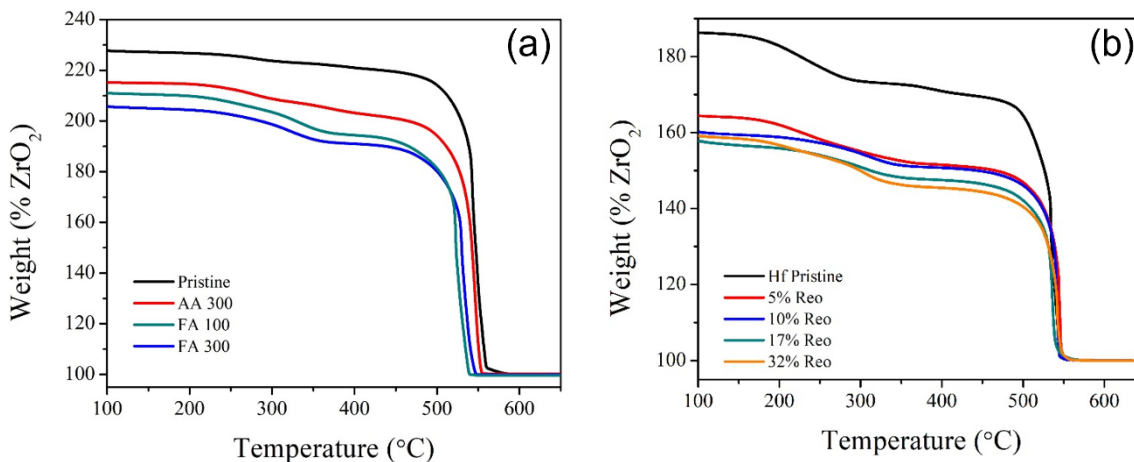**Thermal gravimetric analysis**

Figure S3: Thermogravimetric analysis for Zr-UiO-66 (a) and Hf-UiO-66 (b).

TGA was collected on a TA 5500 thermogravimetric analyzer. For each sample. 10mg was loaded onto a Pt pan and ran from 30 °C to 650 °C with a ramp rate of 10 °C/minute under flowing air. Defect levels were calculated according to published literature procedures.[27]
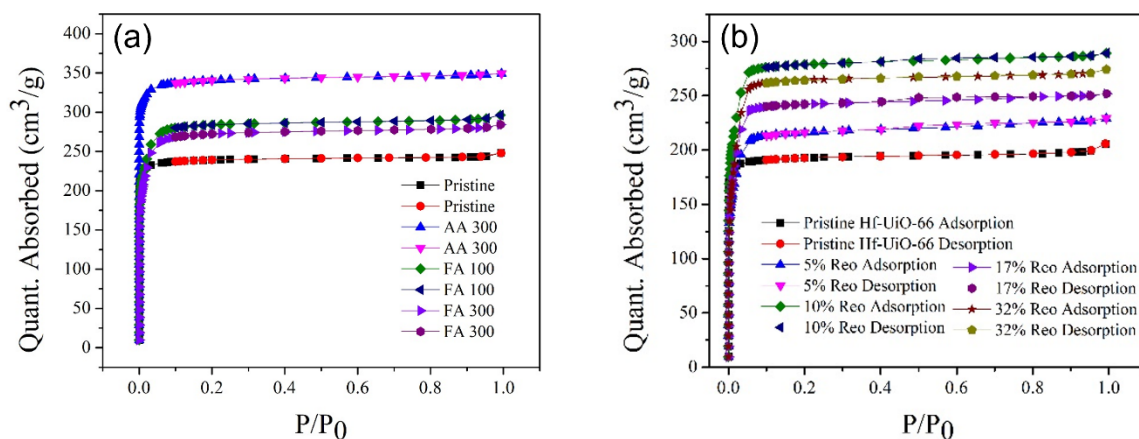
Nitrogen adsorption isotherms

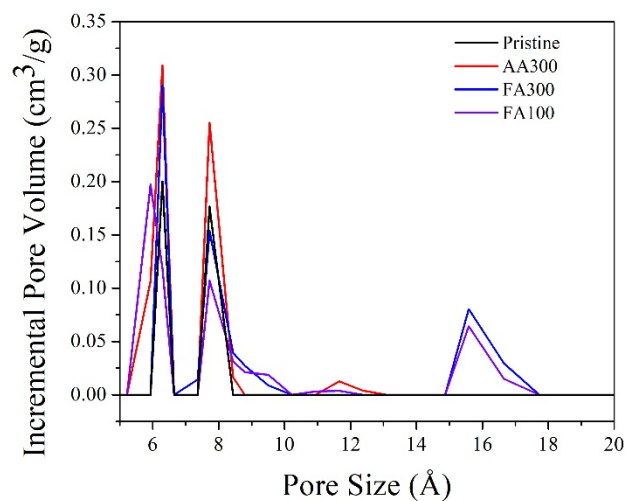**Figure S4**: Nitrogen isotherms for Zr-UiO-66 (a) and Hf-UiO-66 (b) taken at 77 K.

Figure S4: Pore-size distribution for Zr-UiO-66 obtained from N_2 isotherms at 77K.

N_2 isotherms and pore size distribution plots were obtained using a Micromeritics 3Flex adsorption analyzer The samples were activated overnight at 150 °C to remove excess moisture prior to analysis at 77 K.